

Quantum Dot Density Influence upon Coulomb Scattering Rates in Transition Stage and Steady State of QD Laser

Ra'ed M. Hassan

Dept. of Physics, College of Education for Pure Science, University of Basrah, Basrah, IRAQ
raed_m_hassan@yahoo.com

Abstract: In this work, we take into account the semiconductor quantum dot (QD) rate equations based on a microscopic approach which used with a fitting expressions of nonlinear Coulomb scattering rates. The scattering rates play a role in the rate equations of semiconductor QD laser. This paper discussed the influence of different values of the QD density upon the nonlinear Coulomb scattering rates in transition stage and at the steady state of QD laser output. Our results show the dependence of the carrier-carrier scattering rates on both the wetting layer and QD.

[Ra'ed M. Hassan. **Quantum Dot Density Influence upon Coulomb Scattering Rates in Transition Stage and Steady State of QD Laser.** *J Am Sci* 2016;12(1):31-39]. (ISSN: 1545-1003). <http://www.jofamericanscience.org>. 5. doi:[10.7537/marsjas120116.05](https://doi.org/10.7537/marsjas120116.05).

Keywords: Quantum Dot laser, Coulomb Scattering Rates, QD Density, InAs/GaAs laser.

1. Introduction

Laser theories may be developed with various levels of sophistication. The high density of states (DOS) in band structure enhances carrier interactions and causes problems including thermal effects and spectral broadening which lead to the laser performance degradation. The QD has atomic-like quantum properties, such as a discrete energy DOS. So QD lasers having large modulation bandwidth, low threshold current, negligible chirp, high output power and efficiency and little or no temperature-dependence of the threshold current. Furthermore, their emission wavelength can be extended up to the telecom wavelengths of 1.3 μm by varying the size and composition of QDs [1]. This makes the type of lasers very efficient in optical communication applications.

To optimize the design of such QD devices, a better understanding of microscopic interaction of light and QDs is necessary. The turn-on dynamics of the electrically pumped edge emitting QD lasers has already been investigated using rate equations or semiconductor Bloch equations incorporating microscopic energy relaxation times [2]. The discussion of cavity quantum electrodynamics (QED) lasers has been carried out, using rate equation theories [3,4]. From conservation mechanism, the rate equations are a set of ordinary differential equations which describe here the time evolution of the laser microcavity characteristics such as populations and polarizations of the QD and wetting layer (WL) [5,6]. To understand the nonlinear dynamics on a microscopic level, it is necessary to implement Coulomb scattering rates and relaxation times as a function of the WL carrier density. The nonlinear scattering rates play roles in the rate equations of QDs semiconductor lasers. The dependence of the carrier-

carrier scattering rates on both the WL electron/hole density is taken into account as a basic model used in this work [7].

In this work, the study is based on a theoretical model of an electrically pumped QD. The relaxation oscillations theory in semiconductor lasers of QDs based on a microscopic approach is given in refs.[7,8]. We study the nonlinear Coulomb scattering rates relationship for severity of all types of carriers in the cases of pump/lasing states with noting the effect of increasing the QD density of each case. The results present a theoretical simulation of the InAs/GaAs semiconductor QD laser with wavelength of 1.3 μm driven by electrical current pulses.

2. The Theoretical Model

For semiconductor QD laser, one can consider four-level systems which are two for electrons and holes in the WL and another two for electrons and holes in the QDs. Only the energetically lowest electron and hole levels in the QDs contribute crucially to the laser dynamics [5]. Since, the carrier relaxation processes are much faster ($\sim 1\text{ps}$) within the WL and the QD states than capture processes from the WL into the QDs at high WL carrier densities [9]. This is because that the electrons are first injected into a WL before they are captured by the QDs. The energy conservation requires the Auger capture processes for electrons and holes as shown in Figs.1 which illustrating the considered from the scheme of the QD-WL structure [5]. The carrier-carrier scattering processes have an important contribution to the dynamics of QD lasers [10]. The scattering rates and measured scattering times will explain their dependencies upon the WL carrier densities in this work.

One can use the nonlinear rate equations to determine the dynamics of the photon density (\bar{f}_{photon}), the charge-carrier densities in the QDs ($\bar{f}_{QDot}^{e,h}$) and the carrier densities in WL ($\bar{f}_{Wett}^{e,h}$). The Coulomb scattering rates for electron and hole capture processes are function of the respective WL electron and hole densities for different ratio between these densities. Where it is assumed there are ratio, h_{Wett}

between WL carrier densities ($h_{Wett} = \bar{f}_{Wett}^h / \bar{f}_{Wett}^e$). For a better comparison with simplified models choosing a ratio between WL carrier densities in agreement with corresponding stationary values of $\bar{f}_{Wett}^e(t)$ and $\bar{f}_{Wett}^h(t)$, which they represent the numerically evaluated fitted nonlinear Coulomb scattering rates $\zeta_{in}^e, \zeta_{out}^e, \zeta_{in}^h$ and ζ_{out}^h are given by [11].

$$\zeta_{in}^e(t) = b_1 \left[\frac{10}{1 + e^{\frac{38 - \bar{f}_{Wett}^e(t)}{6}}} \right] \left[\frac{e^{\frac{38 - \bar{f}_{Wett}^e(t)}{b_2}}}{1 + e^{\frac{38 - \bar{f}_{Wett}^e(t)}{b_2}}} \right] + 0.012 \times e^{12 \times \frac{[\bar{f}_{Wett}^e(t) - 124.5]^2}{29.6^2}} \dots\dots(1)$$

$$\zeta_{out}^e(t) = e^{\frac{1.73 - \bar{f}_{Wett}^e(t)}{b_3}} + 0.1154 \times e^{\frac{[\bar{f}_{Wett}^e(t) - 27]^2}{137.8}} + [1 - e^{\frac{1 - \bar{f}_{Wett}^e(t)}{2}}] \times e^{\frac{[\bar{f}_{Wett}^e(t)]^2}{b_4}} \dots\dots(2)$$

$$\zeta_{in}^h(t) = \frac{b_5}{171 \sqrt{\frac{\pi}{2}}} \times \text{Tanh}[b_6 \bar{f}_{Wett}^h(t)] \times e^{-2 \frac{[\bar{f}_{Wett}^h(t) - 182]^2}{171.2}} \dots\dots\dots(3)$$

$$\zeta_{out}^h(t) = b_7 [1 - e^{-\frac{\bar{f}_{Wett}^h(t) + 1.2}{1.7}}] \times e^{\frac{[\bar{f}_{Wett}^h(t)]^2}{18854}} + e^{\frac{\bar{f}_{Wett}^h(t) - b_8}{26.4}} \dots\dots\dots(4)$$

where b elements are a eight linear and nonlinear equations;

$$b = \begin{bmatrix} 0.615 & 0.45 & -0.175 \\ 0. & 25.5 & -5. \\ 8. & 0.228 & 0. \\ 0.096 & -0.0095 & 0. \\ 13.4 & -4.85 & 0.718 \\ 963. & -153. & 0. \\ 0.2823 & 0.0201 & 0. \\ -0.9 & -3. & 0. \end{bmatrix} \begin{bmatrix} 1. \\ h_{Wett} \\ h_{Wett}^2 \end{bmatrix} \dots\dots\dots(5)$$

the variables \bar{f}_{Wett}^e and \bar{f}_{Wett}^h have to be inserted in units of 10^{11} cm^{-2} to obtain correct results. These fits have to be used with great care since the dynamic response depends sensitively on the nonlinear scattering rates. One can substitute the in/out-nonlinear Coulomb scattering rates from Eqs.(1)-(4) in rate equations model.

The following nonlinear rate equations for the photon density, $\bar{f}_{photon}(t)$, the charge - carrier densities in the QDs, $\bar{f}_{QDot}^{e,h}(t)$, and the carrier densities in WL, $\bar{f}_{Wett}^{e,h}(t)$ determine the dynamics [7,8]:

$$\dot{\bar{f}}_{photon}(t) = -2k\bar{f}_{photon}(t) + \Gamma U_{indu}(t) + \beta U_{QDot}(t) \dots \dots \dots (6)$$

$$\dot{\bar{f}}_{QDot}^e(t) = -\frac{\bar{f}_{QDot}^e(t)}{\tau_{intr}^e(t)} + \zeta_{in}^e(t)N_{QDot} - U_{indu}(t) - U_{QDot}(t) \dots \dots \dots (7)$$

$$\dot{\bar{f}}_{QDot}^h(t) = -\frac{\bar{f}_{QDot}^h(t)}{\tau_{intr}^h(t)} + \zeta_{in}^h(t)N_{QDot} - U_{indu}(t) - U_{QDot}(t) \dots \dots \dots (8)$$

$$\dot{\bar{f}}_{Wett}^e(t) = \frac{j(t)}{e_o} + \bar{f}_{QDot}^e(t) \frac{N_{Wett}}{\tau_e N_{QDot}} - \zeta_{in}^e(t)N_{Wett} - U_{Wett}(t) \dots \dots \dots (9)$$

$$\dot{\bar{f}}_{Wett}^h(t) = \frac{j(t)}{e_o} + \bar{f}_{QDot}^h(t) \frac{N_{Wett}}{\tau_h N_{QDot}} - \zeta_{in}^h(t)N_{Wett} - U_{Wett}(t) \dots \dots \dots (10)$$

where the coefficient k expresses the total cavity loss or cavity damping, Γ is the optical confinement factor, $j(t)$ is the injection current density, β is the spontaneous emission coupling factor, and $\tau_{intr}^{e,h}(t)$ are the intraband scattering times of electron/hole where

$$\frac{1}{\tau_{intr}^{e,h}(t)} = \zeta_{in}^{e,h}(t) + \zeta_{out}^{e,h}(t) \dots \dots \dots (11)$$

Here $U_{indu}(t)$ is the induced processes rate of absorption and emission, exciting-dominated spontaneous emission in the QD is approximated by bimolecular recombination is modeled by $U_{QDot}(t)$, and $U_{Wett}(t)$ is the WL spontaneous recombination rate;

$$U_{indu}(t) = C_{Einst} A_{Wett} \bar{f}_{photon}(t) [\bar{f}_{QDot}^e(t) + \bar{f}_{QDot}^h(t) - N_{QDot}] \dots \dots \dots (12)$$

$$U_{QDot}(t) = \frac{C_{Einst}}{N_{QDot}} \bar{f}_{QDot}^e(t) \bar{f}_{QDot}^h(t) \dots \dots \dots (13)$$

$$U_{Wett}(t) = \frac{C_{Einst}}{N_{Wett}} \bar{f}_{Wett}^e(t) \bar{f}_{Wett}^h(t) \dots \dots \dots (14)$$

where N_{QDot} denotes the QD density and N_{Wett} is the WL effective density of states, A_{Wett} is the WL normalization area and C_{Einst} is the Einstein coefficient. Both spontaneous emission and induced processes are proportional to the Einstein coefficient [12].

The induced processes of emission and absorption are expressed. For one effective light mode, the carrier-light interaction is considered with the assumption of only single photon number dominating over all other modes [13]. Of QD lasers, the internal losses are adapted to the experimental realization [14] and pump processes are expressed by the injection

current density pulse [15,16]. The spontaneous emission coefficient stands for the probability that the photons generated during the spontaneous emission contribute to the considered laser mode in the cavity [1,12]. Since, the injection current density pulse (the carrier injection into the wetting layer is expressed by the injection current density pulse) divided by the elementary charge e_o , one can use the expression for

current pulse simulation ($j(t) = j_0 e^{-\left(\frac{t-t_0}{\Delta t}\right)^m}$) [8],

where j_0 is the maximum amplitude of current pulse, m is an integer number.

3. The results and discussion

In this work, we focus on the study of the relationship as nonlinear Coulomb scattering rates for severity of all types of carriers in the cases of pump and lasing states with noting the effect of increasing the QD density of each case. In the pump states of InAs/GaAs QD laser at 1.3 μm wave-length at room temperature form figs. 1, we find that the increased WL hole density tend to increase in-electron scattering rate exponentially. This is occurs in the turn-on transition region as shown in Fig. 1(a) which is limited before access to the attractive part in the far-range of WL hole density. In the far-range, the curve will be attractor form which leads to steady state as shown in smallest figures in the Figs. 1. This case of WL hole density is

independent on QD density in the microcavity. While we find that the increase in WL hole density tend to increase in-hole scattering rate as a quasi-linear. We also find that curve in the figure tends to settle at a value ($\sim 40 \text{ ps}^{-1}$) do not change within the attractive after the transit region as shown in Fig. 1(b). Reflected to act with the characteristics of out-carriers Coulomb scattering rate, where land amount is increasing WL hole density as shown in Figs. 2 (c) and (d). We find that land amount out-electron scattering rate versus WL hole density are nonlinear decreasing (approximately a semi-linear between the values (6. -12.) $\times 10^9 \text{ cm}^{-2}$) as shown in Fig. 1(c). The out-hole scattering rate fall exponential as shown in Fig. 1(d), then the end of curve settle at a value (70 ps^{-1}).

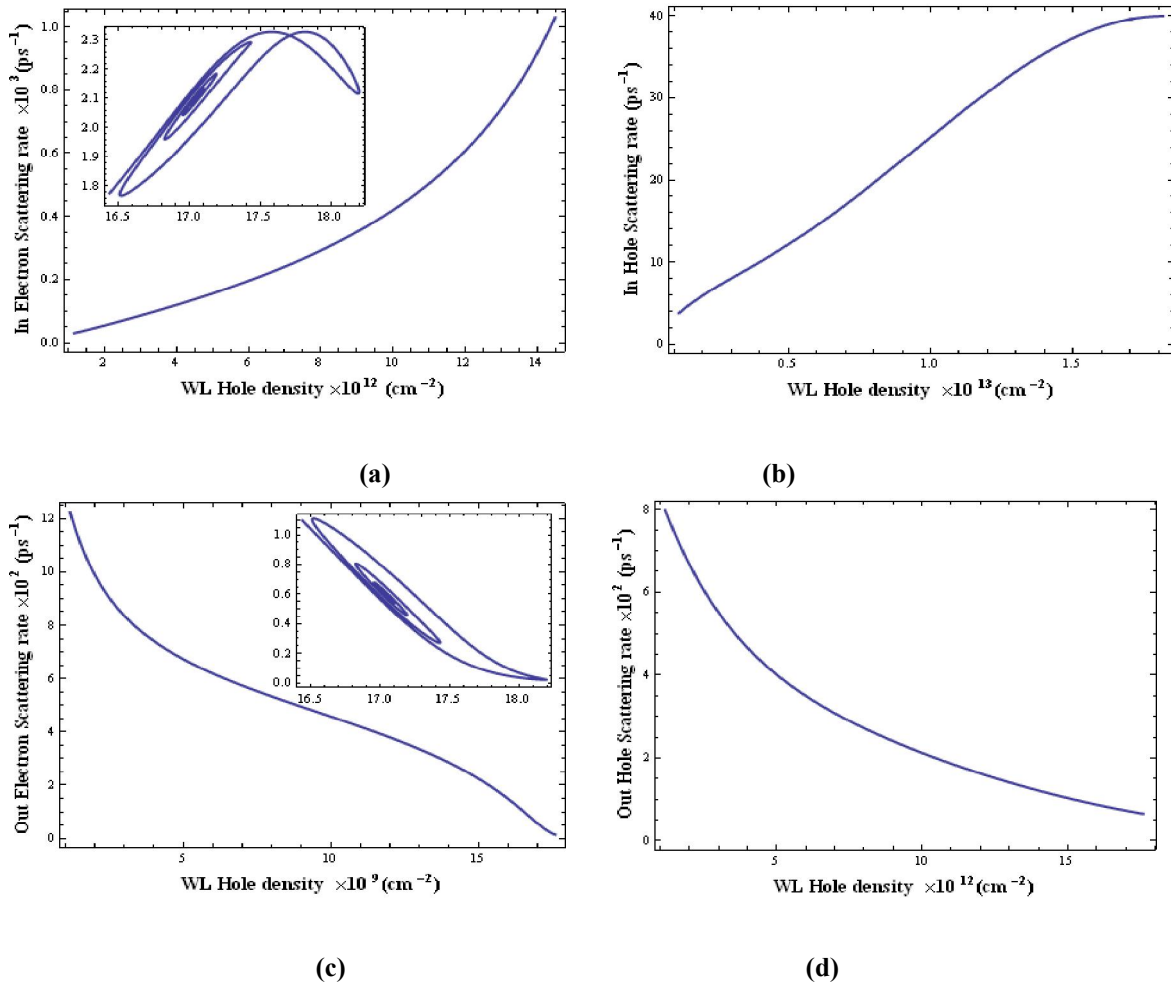


Figure 1: Characteristics of nonlinear carrier scattering rates (left column for electron and right column for hole) in transition stage of InAs/GaAs QD laser at 1.3 μm wave-length vs. the WL hole density: (a) and (b) In scattering rate, (c) and (d) Out scattering rate. The smallest figure is the steady state attractor curve. The parameters used [11]:

$k = 0.12 \text{ ns}^{-1}$, $\Gamma = 0.0015$, $\beta = 5. \times 10^{-6}$, $N_{Wett} = 2. \times 10^{13} \text{ cm}^{-2}$, $A_{Wett} = 4. \times 10^{-5} \text{ cm}^2$, $C_{Einst} = 1.3 \text{ ns}^{-1}$, $J_0 = 4.4986 e_0 \times 10^{13} \text{ cm}^{-2} \text{ ps}^{-1}$, $\Delta t = 2.5 \text{ ns}$, $h_{Wett} = 2.5$. The mini-figures describe the emergence of attractive in large ranges of density of WL carriers.

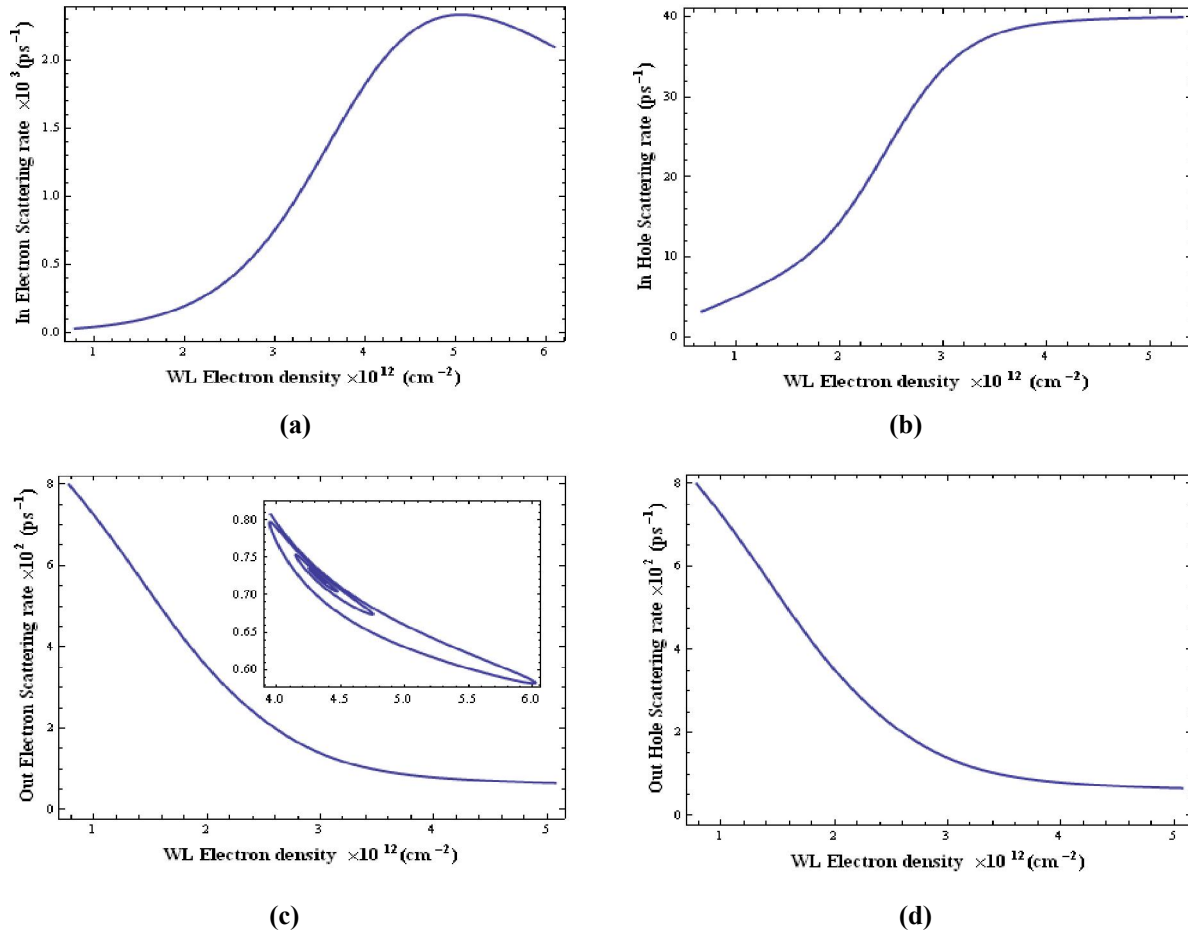


Figure 2: Characteristics of nonlinear carrier scattering rates (left column for electron and right column for hole) in transition stage of InAs/GaAs QD laser at 1.3 μm wave-length vs. the WL electron density: (a) and (b) In scattering rate, (c) and (d) Out scattering rate. The mini-figures describe the emergence of attractive in large ranges of density of WL electron.

Study the effect of WL electron density in nonlinear Coulomb scattering rate is studied from Figs. 2 depends on the QD density in the microcavity. In Figs. 3(a) and (b), we can understand how the increase in in-scattering rate with increasing WL electron density. The impact of this factor leads to an exponential increase in-electron scattering rate, then at least increase the scattering rate reaches to the greatest value ($\sim 2325 \text{ ps}^{-1}$), and appears to be drop the scattering rate to the value ($\sim 2150 \text{ ps}^{-1}$) at WL electron density value ($\sim 6 \times 10^{12} \text{ cm}^{-2}$) before returning into an attractive region which save the curve bath. In Fig. 2(b), we can see a left side of semi-Gaussian growth of the in-hole scattering rate with increasing WL electron

density. Which tend to settle at ($\sim 40 \text{ ps}^{-1}$) even up to the WL electron density value ($\sim 6 \times 10^{12} \text{ cm}^{-2}$). That returnee into an attractive and repeated the same conduct in the Fig. 2(a). Properties of nonlinear out-scattering rate in lasing states are as the same in Figs. 1(c) and (d). The amount of out-electron scattering rate fall with increase WL electron density to be stabilized at values close to zero before entering into attractive region as shown in Fig. 2(c). At the same time, the out-electron scattering rate would be like a right side of semi-Gaussian decreasing to reach the value ($\sim 1225 \text{ ps}^{-1}$). This is clearly shows that the effect of this factor is entering the curve into attractive region at WL electron density value ($\sim 6 \times 10^9 \text{ cm}^{-2}$) as shown in Fig. 2 (c).

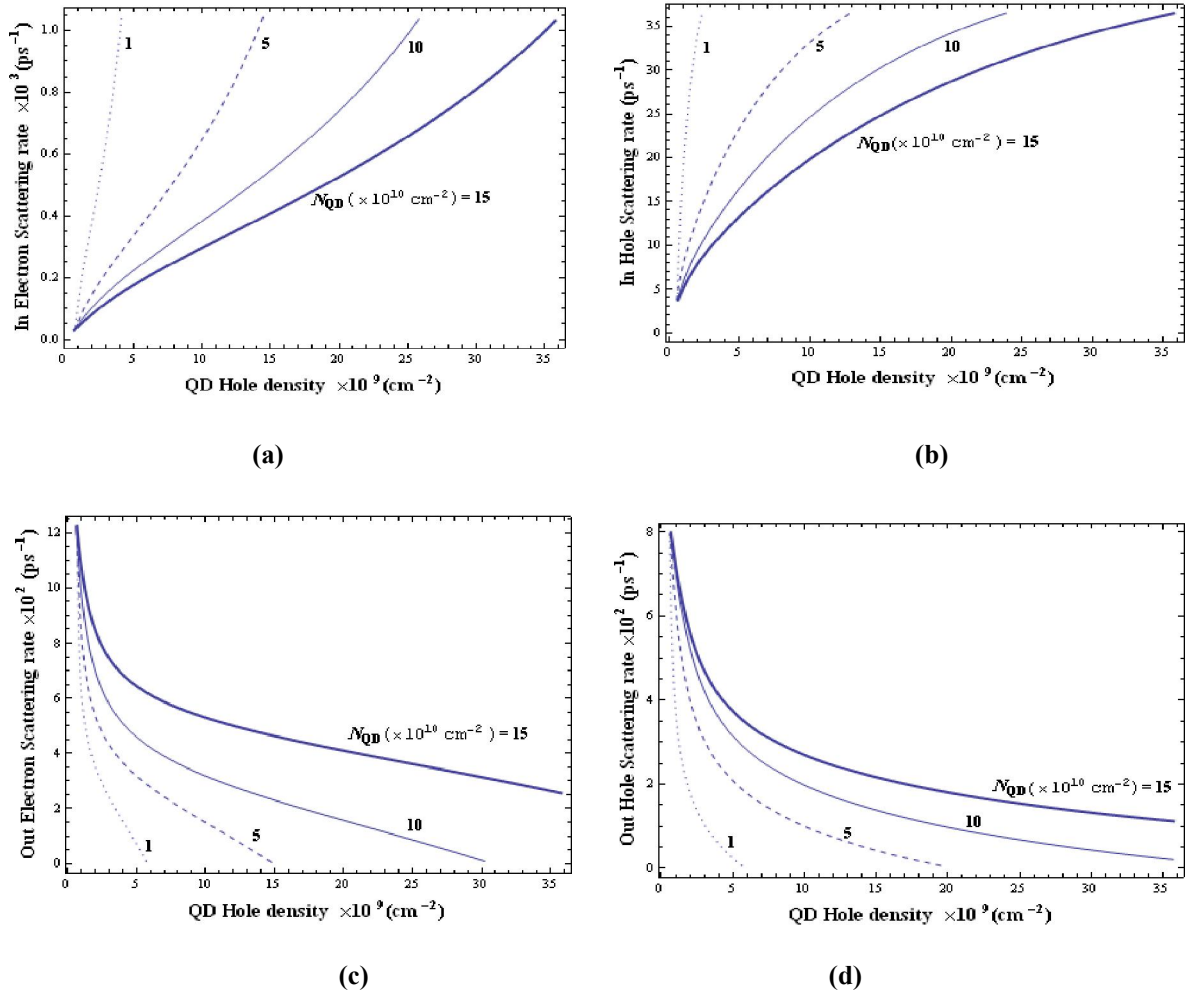


Figure 3: Characteristics of nonlinear carrier scattering rates (left column for electron and right column for hole) in transition stage of InAs/GaAs QD laser at 1.3 μm wave-length vs. the QD hole density: (a) and (b) In scattering rate, (c) and (d) Out scattering rate. For different value of the QD density, $N_{QDot} (\times 10^{10} \text{ cm}^{-2}) = 1$ (dotted curve), = 5 (dashed curve), = 10 (thin curve), = 15 (thick curve).

Logically, The changing in QD density play a role in the quantity of Coulomb scattering rate, that has been shown from its impact on the density of carriers in the QD as noted in the theoretical results appear in the Figs. 3 and 4. The relationship between the severity of in-carriers Coulomb scattering rate change and QD hole density shown in Figs. 3(a) and (b). That disposal is almost similar the change of WL hole density for the phenomenon in Figs. 2(a) and (b). The different in these figures is the relationship is supported by the QD density which is characterized by declining the curves with the increase in the number of QD (taken different curves within the QD density: 1, 5, 10 and 15 ($\times 10^{10} \text{ cm}^{-2}$)). So the increasing of this factor will work to

inhibit the amount of nonlinear scattering and makes an attractive beginning of steady state located within far QD hole density. This effect is repeated with out-carriers Coulomb scattering rate but in reversible behavior as shown in Figs. 3(c) and (d). In these figures, the increase in the number of QD will increase the nonlinear scattering rate with the change of QD hole density. The amount of any decline curves decreases with increasing this factor. The QD carrier's density and nonlinear Coulomb scattering rates at the steady state for different QD density are exact amounts as ordered in the Table (1). So we can calculate the intraband scattering times of electron/hole.

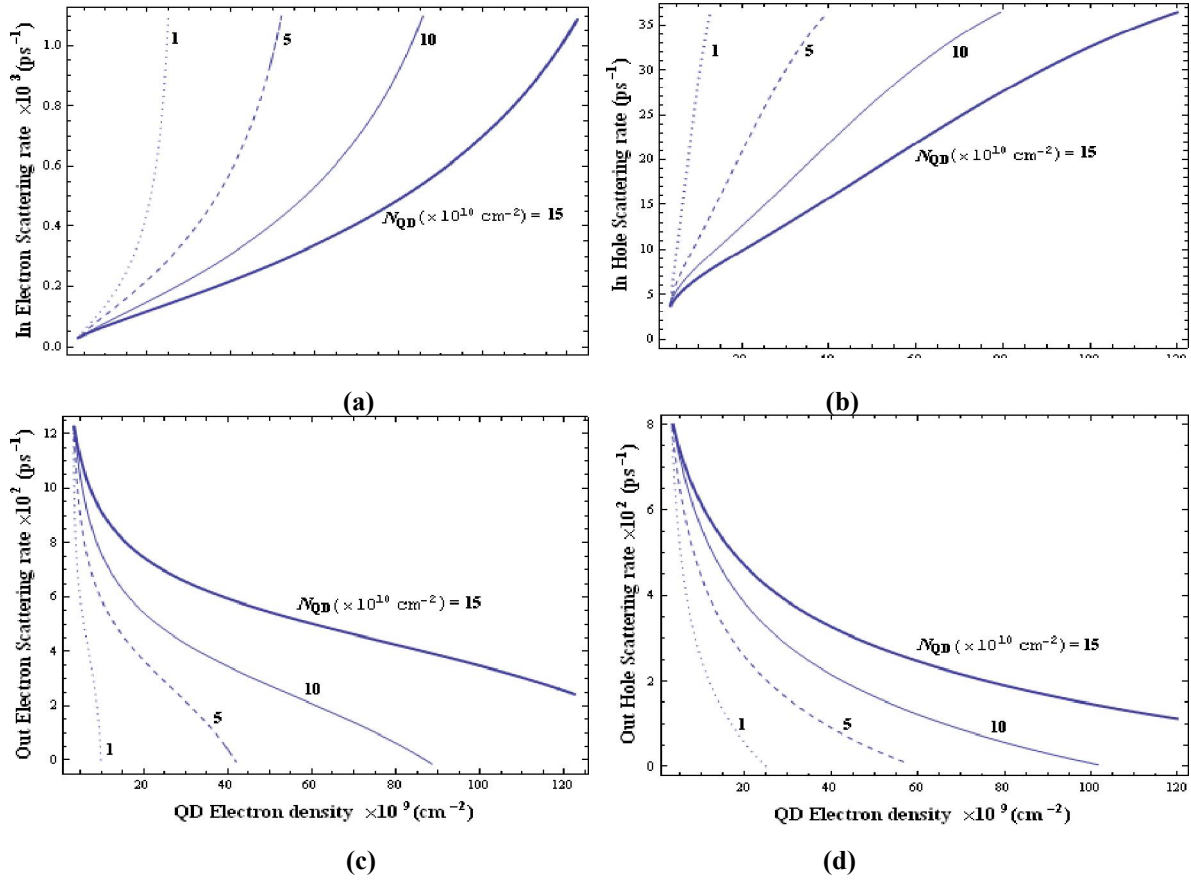


Figure 4: Characteristics of nonlinear carrier scattering rates (left column for electron and right column for hole) in transition stage of InAs/GaAs QD laser at 1.3 μm wave-length vs. the QD electron density for different value of the QD density: (a) and (b) In scattering rate, (c) and (d) Out scattering rate.

The results show that the influences of a similar group by the exact amount to reduce the effect of QD electron density increase on in-electron/hole scattering rate as shown in Figs. 4 (a) and (b). While that decreasing the impact on out- electron/hole scattering

rate (see Figs. 4(c) and (d)). That will make the steady state attractive in a far beyond of the QD electron density. This means that nonlinear scattering rates go to different values limits depending on the QD density in the microcavity.

Table 1: QD carriers density and Scattering rates at the steady state for different QD density.

$N_{Qdot} \times 10^{10}$ (cm^{-2})	$\bar{f}_{QDot}^e \times 10^9$ (cm^{-2})	$\bar{f}_{QDot}^h \times 10^9$ (cm^{-2})	ζ_{in}^e (ps^{-1})	ζ_{in}^h (ps^{-1})	ζ_{out}^e (ps^{-1})	ζ_{out}^h (ps^{-1})
1	9.713	3.356	2099	39.74	59.57	72.6
5	40.89	12.18	1089	37.06	241.8	106.2
10	79.75	23.35	1025	36.52	257.5	111.5
15	118.6	34.5	1000	36.41	263.1	112.9

The chosen initial conditions the system can access an attractor. It is important to note that the center of the spiral motion of the trajectory in Fig. 6, representing the regular intensity pulsations, does not match with the steady state densities.

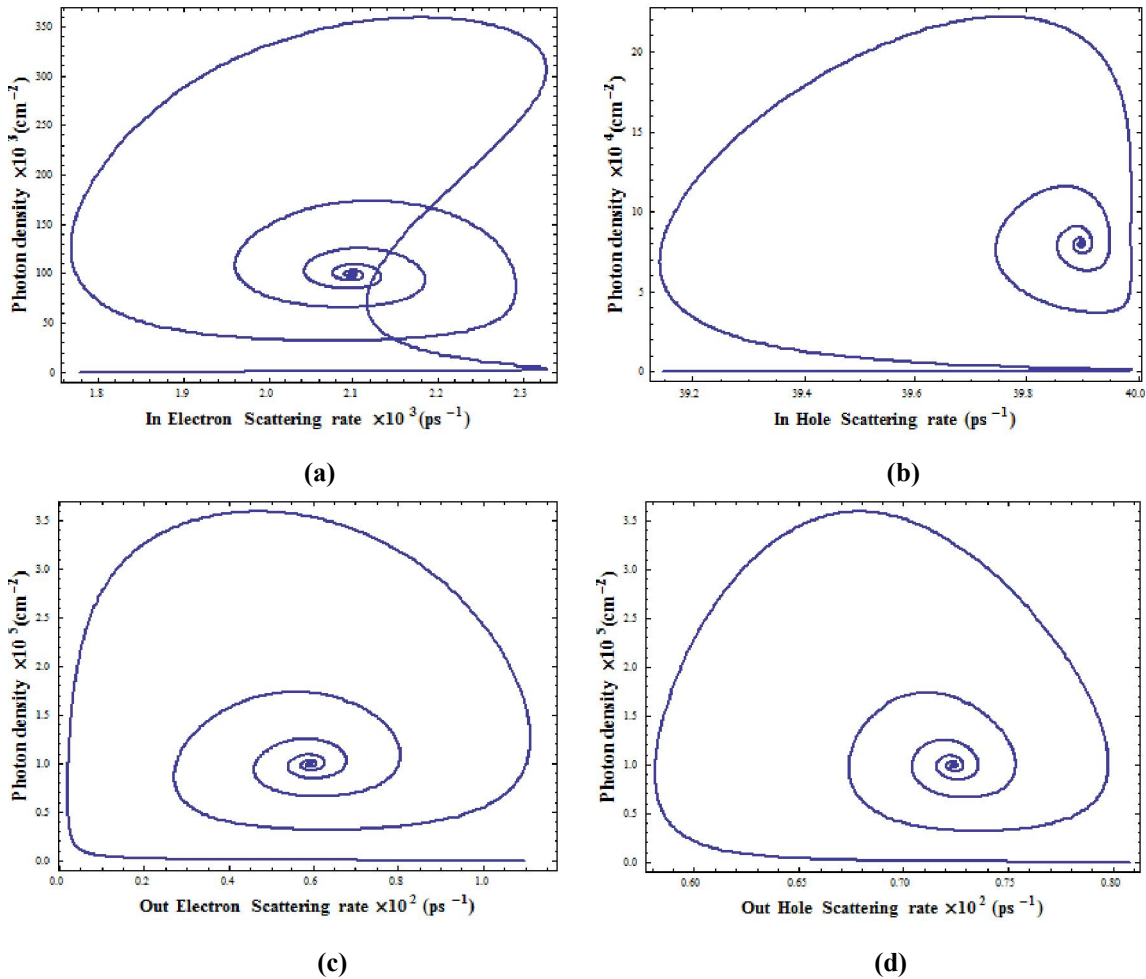


Figure 5. Phase space projections of the trajectory onto planes spanned by the photon density n_{ph} and the nonlinear carrier scattering rates of InAs/GaAs QD laser vs. the WL electron density: (a) and (b) In scattering rate, (c) and (d) Out scattering rate.

4. Conclusion

The QD density is one of the most important factors affecting the efficiency of the laser QD. In this work, we find that the increase of this factor does not affect the density of WL carrier's density of InAs/GaAs QD laser at 1.3 μm wave-length at room temperature. We display the increase of QD density dose affect in a microcavity which do increase the QD carrier's density. The characteristics of nonlinear Coulomb scattering rate are affected greatly by it depending on the amount of QD density. Qualitative responses of scattering rates are different. The theoretical results find that out-carriers (electron / hole) scattering rate and in-hole scattering rate increases with increase of this density unevenly, but in-electron scattering rate decreases.

References

1. P. Michler. "Single Semiconductor Quantum Dots". © Springer, Hardcover, (2009).
2. J. E. Kim, E. Malic', M. Richter, A. Wilms, and A. Knorr. IEEE Journal of Quantum Electronics, 46(7):1115-1126, (2010).
3. Pierre Meystre and Murray Sargent III. "Elements of Quantum Optics". ©Springer-Verlag Berlin Heidelberg, (2007).
4. Marian Florescu and Sajeev John. Physical Review A, 69: 053810(1-21), (2004).
5. T. R. Nielsen, P. Gartner, and F. Jahnke. Physical Review B, 69: 235314(1-13), (2004).
6. Tey Meng Khoon. PhD. thesis, Department of Physics, National University of Singapore, Singapore, (2008).

7. Ermin Malić, Moritz J. P. Bormann, Philipp Hövel, Matthias Kuntz, Dieter Bimberg, Andreas Knorr, and Eckehard Schöll. IEEE Journal of Selected Topics in Quantum Electronics, 13(5): 1242- 1248, (2007).
8. Kathy Lüdge, Moritz J. P. Bormann, Ermin Malić, Philipp Hövel, Matthias Kuntz, Dieter Bimberg, Andreas Knorr, and Eckehard Schöll. Physical Review B, 78: 035316(1-11), (2008).
9. R. Wetzler, A. Wacker, and E. Schöll. Journal of Applied Physics, 95(12): 7966 - 7970, (2004).
10. Paul Harrison. "*Quantum Wells, Wires and Dots: Theoretical and Computational Physics of Semiconductor Nanostructures*". ©John Wiley & Sons Ltd., The Atrium Southern Gate, Chichester, (2005).
11. R. M. Hassan, PhD thesis. "*Turn-on Dynamics and Lasing Operation Characteristics of Semiconductor Quantum Dot Lasers*". University of Basrah, (2011).
12. Emmanuel Rosencher and Borge Vinter. "*Optoelectronics*". ©Cambridge University Press, English edition (2004).
13. Janik Wolters, Matthias-René Dachner, Ermin Malić, Marten Richter, Ulrike Woggon, and Andreas Knorr. Physical Review B, 80: 245401(1-7), (2009).
14. Matthias Kuntz. PhD. thesis, Technische Universität Berlin, Berlin, Germany, (2006).
15. P. G. Eliseev, H. Li, G. T. Liu, A. Stintz, T. C. Newell, L. F. Lester, and K. J. Malloy. IEEE Journal of Selected Topics in Quantum Electronics, 7(2): 135-142, (2001).
16. Levon V. Asryan and Serge Luryi. IEEE Journal of Quantum Electronics, 40(7): 833-843, (2004).

12/20/2015